Spatio-Temporal Complexity in Nonlinear Image Processing

JAMES P. CRUTCHFIELD

Abstract—**This is a pictorial survey of pattern dynamics in video feedback and in related numerical models. After a short introduction to video feedback apparatus and concepts from dynamical systems theory, a range of phenomena are presented, from simple attractor types to homogeneous video turbulence. Examples of complex behavior include symmetry-locking chaos, spatial amplification of fluctuations in open flows, dislocations, phyllotaxis, spiral waves, and noise-driven oscillations. Video experiments on nonlinear transformations of the plane are also described. The survey closes with a discussion of the relationship between dynamical systems and nonlinear, iterative image processing.**

Keywords—**Attractor, basin, chaos, coherence, complexity, dimension, dislocations, entropy, flows, image processing, lattice dynamical systems, limit cycle, mappings, partial differential equations, phyllotaxis, reaction-diffusion, spatially extended systems, spiral waves, transients, turbulence, video feedback.**

I. Introduction

CHAOS is now the most notorious [1] and well-studied [2], [3] source of complex behavior arising in nonlinear deterministic processes. The specific complexity-generating mechanisms referred to under this rubric are not the entire story, however. As the following pictorial survey will demonstrate, complexity in spatio-temporal systems demands substantial generalizations to the basic theory of dynamical systems and to our present appreciation of the diverse forms manifested by the interplay of randomness and order. Although chaos is only one of many complex phenomena, the rapid progress made in its understanding gives hope that the diversity of spatio-temporal behavior will also yield to a similar "experimental mathematical" approach [4].

Indeed, the particular spatial systems presented in the following, video feedback [5] and lattice dynamical systems [6], were taken up in order to address the larger questions of just how dynamical systems theory, as developed for understanding low-dimensional chaos, could be applied to a wider range of physical processes, viz. those whose behavior depends on time and on space. Along the way a number of new phenomena and connections with well-known behavior were discovered. This pictorial survey is concerned with this phenomenology as it appears in two spatial dimensions. First, though, basic notions from dynamical systems and the apparatus of video feedback must be introduced. After presenting a range of different phenomena in video feedback and related numerical models, the discussion closes by addressing several general questions of interest to engineering. Specifically, the last section considers the relevance of the experimental-mathematical approach to the "engineering" of nonlinear image processing systems.

Manuscript received September 10, 1987. This work was supported in part by the Office of Naval Research under Grant N00014-86-K-0154. The numerical simulations were performed on a Cray X/MP and on a Sun Microsystem workstation with a Mercury Computer Systems ZIP 3232 array processor. The former was funded by the Cray-Sponsored University Research and Development Grant Program.

The author is with the Physics Department, University of California, Berkeley, CA 94720.

IEEE Log Number 8821323.

II. Video Feedback

Space does not allow a detailed introduction to the topics covered in the following sections (the reader is referred to a paper [5] and references therein, and to a videotape [7] for this). In the former, a more complete discussion of the experiments and related video physics is presented. In the latter, excerpts from various experiments can be seen evolving in time. Since one of the major focal points is the complexity of time-dependent behavior, the videotape is a substantial improvement over the static images required by a conventional publication format. An even better approach is for the reader to experiment with video feedback directly, which is highly encouraged. Although scientific experimentation requires careful calibration and instrumentation quality equipment, most of the phenomena described below can be observed in consumer grade video equipment with patient investigation. For an introduction to *lattice dynamical systems*, a class of numerical models that evolved out of the video feedback investigations, see [6].

The basic configuration of a video feedback system is quite simple. When a video camera is directed at a display monitor, to which it is connected, a feedback loop is closed. Two-dimensional images $I(x, y)$ from the monitor screen impinge on the camera's photodetector after passing through space and optical processing elements. The camera dissects the image into an electronic signal $V(t)$ by *raster* scanning the intensity profile on the photodetector into a temporal sequence of horizontal lines. The video signal $V(t)$ gives the intensity of a point, or pixel, along a raster scan line at time t. The signal arrives at the monitor after electronic processing and is reconstructed as a two-dimensional image on its screen. Thus as it flows around the loop, there are two domains in which the image information can be processed: optical and electronic.

Optical image processing often consists passing the image through various lens systems that control the light inten-

0098-4094/88/0700-0770$01.00 ©1988 IEEE

sity gain (iris), image focus, and spatial magnification and filtering. There might also be nonlocal image processing, such as image translation or rotation. The latter can be effected by mounting the camera so that it rotates about its optical axis. Electronic processing provides spatially local image processing as it operates directly on the instantaneous intensity signal $V(t)$, that is, on horizontal and possibly vertical pixel neighborhoods. Electronic image processors provide modules to handle the basic video frame and line synchronization, to add and multiply images point by point, and to perform nonlinear pixel and pixel neighborhood transformations [8]. Spatially nonlocal electronic image processing can be performed by manipulating the raster geometry itself and displaying the result on a suitably modified monitor [9].

A question that frequently arises in using electronic systems to investigate theoretical problems of complexity is whether the process involved is a simulation or an experiment. The distinction is somewhat moot as long as science is served. Nonetheless, it should be said that once the functional elements are well characterized, video feedback as an experiment becomes video feedback as simulation. This is simply a change in the experimenter's attitude rather than in the apparatus or the phenomena observed. Speaking broadly, as a simulator video feedback allows one to study the class of systems, called *reaction-diffusion partial differential equations* introduced by Alan Turing [10]. It can do much more than this, though, such as simulate spin glasses, neutral networks, delay-partial-differential equations, multi-species chemical reactions, and so on. Discussion of these systems is beyond this survey's scope.

III. Dynamical Systems

A central motivation in studying video feedback has been to understand how the geometric picture and statistical methods of dynamical systems theory can be generalized to explain the complexity observed in time-dependent pattern generating systems. Thus to put the investigation in the proper framework, the following section introduces a few notions from dynamical systems theory [2], [3] that will be used later on.

The primary abstraction of dynamical systems theory is that the instantaneous configuration of a process is represented as a point, or **state,** in a space of states. The dimension of the space is the number of numbers required to uniquely specify the configuration of the process at each instant. With this, the temporal evolution of the process becomes the motion from state to state along an **orbit** or **trajectory** in the state space.

For video feedback the space of states is the space of two-spatial-dimension patterns $I(x, y)$. For a monochrome system $I(x, y)$ is the intensity at a point (x, y) on the screen; for color, I consists of a vector of red, green, and blue intensity components. The dimension of the equivalent dynamical system is given by the effective number of pixels. For the behavior described below a (rough) upper bound of the dimension of the state space is 250 000 ($\approx 512^2$). The temporal evolution of patterns is thus abstractly associated with a trajectory in this high-dimensional state space. If the behavior is simple, however, then the trajectory can be pictured as moving in a much lower dimensional subspace.

If a temporal sequence of patterns is observed to be stable under perturbations, then we assume that the trajectory lies on some **attractor** in pattern space. One of the main contributions of dynamical systems theory[1] is the categorization of all long-term behavior into three attractor classes: fixed point, limit cycle, and chaotic attractors. A **fixed point** attractor is a single, isolated state toward which all neighboring states evolve. A **limit cycle** is a sequence of states that are repetitively visited. One can also have a "product" of limit cycle oscillators, called a **torus** and denoted T^n where n is the number of constituent cycles. These attractors describe predictable behavior: two nearby states on such an attractor stay close as they evolve. Unpredictable behavior, for which the latter property is not true, is described by **chaotic attractors.** These are often defined negatively as attractors that are neither fixed points, limit cycles, nor tori.

Aside from attractor classification, another significant contribution of dynamical systems theory is a geometric picture of how transients relax onto the attractors. An attractor's **basin of attraction** is the set of all points that evolve onto the attractor. There can be multiple basins and attractors, so that radically different behavior may be seen depending on the initial configuration. The complete catalog of attractors and their basins for a given dynamical system is called its **attractor-basin portrait.**

Finally, dynamical systems theory is also the study of how attractors and basin structures change with the variation of external control parameters. A **bifurcation** occurs if, with the smooth variation of a control, the attractor-basin portrait changes qualitatively.

To summarize, dynamical systems theory is a language that describes how complexity arises in (i) asymptotic behavior, (ii) basin structure, and (iii) bifurcations. It forms a natural framework with which to explore the complex spatio-temporal dynamics of video feedback. The pictorial essay which follows is organized along the particular phenomena that have been observed in video feedback. The sections are more or less independent.

IV. Basic Spatio-Temporal Attractor Types

This section demonstrates the basic attractor types: fixed points as time-independent equilibrium patterns, limit cycles as periodic image sequences, and a chaotic attractor arising from the competition of marginally stable symmetries.

Photo 1 shows a time-independent and stable pattern. The dynamical system description of this is a fixed point in the space of patterns. Although there are very simple fixed point patterns, such as an entirely dark image, the one shown is complex. This emphasizes an important

[1] Only dissipative dynamical systems will be described here.

distinction with conventional theory in which one does not associate any intrinsic complexity with a fixed point. In the case of spatially-extended systems, measuring the complexity even of fixed points is clearly desirable. Quantification of spatial complexity, however, is fraught with difficulties at present.

Photos 2, 3 and 4 give three snapshots during one cycle of a periodic sequence of patterns. This is a limit cycle in pattern space and is stable under small perturbations.

Photos 5 through 8 show a sequence of snapshots from an aperiodic image sequence. Here there are two marginally stable patterns of fourfold and 21-fold symmetries. The trajectory visits neighborhoods of these patterns intermittently. Analysis of the time-dependent Fourier amplitudes of the underlying symmetric pattern shows the behavior is described by low-dimensional dynamics and is globally stable, and that starting from nearby patterns orbits separate rapidly. Thus, the behavior is most likely described by a chaotic attractor, although the (necessary) measurement of the metric entropy has yet to be carried out.

V. Dislocation Dynamics

Photos 9 and 10 show the interdigitated light and dark fingers of video dislocations. Similar patterns occur in a wide range of physical and biological systems, such as:

(1) convection cell patterns found in Rayleigh–Bénard and Couette fluid flows and in liquid crystal flows;
(2) domains in two-dimensional (anisotropic) spin systems, such as thin magnets used for magnetic bubble devices;
(3) labyrinthine patterns in ferrofluids;
(4) flux patterns in type II superconductors; and
(5) the ocular dominance pattern in the visual cortex.

While the particular mechanisms responsible for dislocations in these examples differ greatly, there is a common element. In each there is an "order parameter" that alternates between saturation extremes over some fixed spatial length scale. The order parameter in each of the examples above is (1) the direction of fluid flow, charge transport, or (2) local magnetization; (3) the existence or absence of ferrofluid; (4) the local conductivity, and (5) the variation of left or right visual field associated with cortex columns.

The diversity of examples calls for a general definition of dislocations. They can be defined as the localized defects arising from the breaking of a pattern's underlying spatial symmetry. The patterns that exhibit the exact symmetry are the "ground" or "vacuum" states. The lowest energy perturbations from these equilibrium states are dislocations.

A wide range of dislocation dynamics is readily observed. In the typical evolution from a random initial pattern, the system first establishes the characteristic spatial wavelength and produces a tangle of "frustrated" fingers with many dislocations. The dislocations collide and annihilate and the pattern becomes more regular. At this point the system may continue to evolve toward less complex patterns or it may begin to spontaneously create dislocations. In the former case, the attractor is a fixed point reached by a complex transient. In the latter case, the attractor manifests itself as a pattern sequence of a "gas" of capriciously-moving dislocations, whose creation and annihilation rates balance. One of the interesting questions here is how to describe the underlying state space structures [11].

Dislocations result from the interplay of two processes. The first is the local bistability of the order parameter. Values of the order parameter intermediate between the saturation extremes are unstable. The second is "lateral inhibition", to borrow a phrase from neurophysiology. This imposes the spatial length scale over which the order parameter alternates by forcing neighbors bordering a region into the opposite saturation state from the region itself.

In video feedback, dislocations are found when using photoconductor-based cameras at high beam current. It appears that secondary electrons are scattered from the beam spot to neighboring regions. In a relative sense, this reduces photosensitivity in those regions when the beam scans illuminated photoconductor and increases it when the beam scans dark photoconductor.

A simple numerical model of dislocations that embodies these processes is given by the following discrete time and space *lattice dynamical system* [6]:

$$x_{n+1}^{\vec{i}} = f\left(\sum_{\vec{j} \in \vec{N}(\vec{i})} c_{\vec{j}} x_n^{\vec{i}+\vec{j}} \right)$$

where

$x_n^{\vec{i}} \in [0,1]$	is the state a site $\vec{i}$ at time n;
$\vec{i} = \{i_0, \cdots, i_{d-1}\}$	indexes the site in a d-dimensional lattice;
$\vec{j}$	is a relative index to the neighboring sites $\vec{N}(\vec{i})$;
$c_{\vec{j}}$	are the coupling kernel coefficients which control the lateral inhibition and set the finger width. For site $\vec{i}$ and possibly its near neighbors, the coefficients are positive. This gives a diffusive coupling. For sites further away, the coefficients are negative which gives inhibitory coupling;
$f(x) = x - k \sin(2\pi x)$	for $k > 0$ gives the stable saturation values of $x = 0$ and $x = 1$. This function is related to the widely studied map of the circle [2].

Photos 11, 12, and 13 show the relaxation from a random initial pattern in a $d = 2$ lattice after 20, 100, and 1100 iterations. Here a 90° rotation of the image is performed on each iteration by a suitably chosen nonlocal neighborhood $\vec{N}$. The system ultimately relaxes, through

the collision and annihilation of dislocations, onto a fixed point attractor consisting of concentric rings.

VI. Coupled Relaxation Oscillators

Many physical, chemical, biological, and engineering systems can be described as coupled relaxation oscillators. Each oscillator plays the role of a local clock: counting up and resetting to some reference state. While the coupling communicates the local phase information to accelerate or retard neighboring oscillators. This section illustrates some of the spatio-temporal patterns that can emerge from this combination: spiral waves and transient spatial chaos.

Spiral waves occur in an active medium with periodic local dynamics diffusively coupled. The most famous example of this behavior is the Belousov–Zhabotinsky chemical reaction [12]. Photos 14, 15, and 16 show the center of three different spiral waves with one, two, and three spiral arms [13] found in video feedback experiments. Dynamically every point in the pattern has a well-defined oscillation phase except for the spiral center where there is a phase singularity. In each photo the distinct colors label stages of the local oscillations.

The second example is a model of a water layer dripping from a flat surface. The equations of motion are similar to that for the dislocation model, except there is simple spatial averaging (all c_j = constant) and the local piecewise-linear dynamics is $f(x) = \omega + sx \pmod 1$. The parameter ω gives the increment in the local variable on each iteration. This determines, if $s = 1$, the clock's period. The parameter s controls the slope which determines the clock's stability: if $s < 1$ the cycles will be stable. The (mod 1) operation performs the resetting or dripping of a thick region of the water layer.

Photos 17 and 18 show the patterns after 310 and 492 steps starting from a uniform pattern with the center site slightly perturbed, and from a random initial pattern, respectively. Although these patterns appear complex, eventually both decay to simple periodic behavior. Thus the observed complexity is only a transient. The surprising result is that for this very simple system the length of the transients grows hyper-exponentially with increasing system size [11]. This is somewhat disturbing since one would have to wait, for the examples shown here, many universe lifetimes to observe the system's attractor. This is a clear example of spatio-temporal complexity that is not described by a chaotic attractor.

VII. Logarithmic Spirals and Phyllotaxis

A common large-scale symmetry found in video feedback patterns is the logarithmic spiral illustrated by Photo 19. This is a natural consequence of camera rotation and optical demagnification. On each circuit of the feedback loop the image is rotated and reduced in size, leading to a sea-shell-like self-similarity.

Biological patterns appear in other regimes as well. Photos 20 and 21 show "crystalline" lattices of stable, isolated dots. In the first the dots at the center fall into a phyllotaxic symmetry. Phyllotaxis refers to the arrangement of leaves on a stem or florets in a composite flower, such as a sunflower, along logarithmic spirals. The second photo (21) illustrates a more complex lattice with domains of simple symmetries separated by walls.

VIII. Open Flows and the Spatial Amplification of Fluctuations

There is a wide class of physical phenomena in which material transport through a system leads to the spatial magnification of small fluctuations. This in turn results in complex macroscopic structure downstream. Open flows, such as pipe flow, are the most well-known examples of this [14]. The structures formed downstream, such as vortex streets or turbulent plugs, are supported in a sense only by the fluctuations: the ideal noiseless systems admit regular flows.

This class of systems is easily studied with video feedback by simply offsetting the camera and monitor centers. With the camera unrotated and offset upwards, for example, successive images are seen displaced downwards on the monitor. When nonlinear electronic processing is added and the local dynamics becomes unstable small fluctuations at the screen top are magnified and propagate down the screen. Photos 22, 23, and 24 show a "waterfall" where perturbations propagate down the screen. The first photo 22 shows the initial development from a small fluctuation on the photo's right side. The second (23) and third (24) photos show its growth and propagation downscreen.

Photos 25 and 26 illustrate another example of how small fluctuations are filtered into manifesting themselves as structured macroscopic patterns. In this situation noise drives relaxation-type oscillations. Here large spatial magnification and light gain make the video system sensitive to small fluctuations. If of sufficient size, the fluctuations are amplified and filtered spatially and temporally to macroscopic observable patterns. Typically, only a few "amplification" pathways are seen; two of which are shown in the photos.

IX. Bifurcations

The foregoing survey has concentrated on the wealth of pattern dynamics arising at particular control settings. Video feedback, much like any analog computer, does not reveal its unique benefits as a real-time investigative tool until one realizes all this phenomenology can be interactively changed and the results immediately seen. This leads to the study of bifurcations through which qualitative changes in the dynamics occur with the smooth variation of control parameters.

9.1. Symmetry Locking and Chaos

The majority of patterns seen so far have exhibited azimuthal symmetry which has been imposed on the image by camera rotation. The ninefold symmetry seen in the video dislocation photos corresponds to a camera rotation of 40 degrees. The effect camera rotation has on behavior can be studied in isolation in the following way. First, the

nonlinear electronic processing is simplified so that it clips to black and white values. Second and more importantly, radial pattern motion can be suppressed by imposing annular boundary conditions with an annular mask centered about the camera-monitor optical axis. This leads to a nearly one-dimensional channel with periodic boundary conditions.

With this setup the camera can be rotated and the effect of the imposed azimuthal symmetries studied systematically. In the language of dynamical systems, the camera angle is the control parameter and we are investigating the bifurcations between stable symmetric patterns. To take a simple example, when the camera is rotated 90 degrees the pattern must have an overall four-fold symmetry. Similarly, for 120 degrees, there is a three-fold symmetry. Thus, there must be a bifurcation between these stable symmetric patterns as the camera angle is varied from 90 to 120 degrees.

Photos 27 through 31 show a bifurcation sequence of patterns as the angle is increased quasistatically through approximately 10 degrees. The first (photo 27) exhibits a five-fold symmetry that rotates counter-clockwise. The second (photo 28) is taken at an angle of 72 degrees. It is stationary and also shows a five-fold symmetry as expected. The third (photo 29) has the same symmetry but rotates clockwise. The fourth photo (photo 30) shows an unstable pattern at the angle of bifurcation. At larger angle, a stable thirteen-fold pattern appears (photo 31).

9.2. *Transition to Fully Developed Video Turbulence*

One of the motivating physical problems for nonlinear dynamics has been the nature of fluid turbulence. While low-dimensional chaotic behavior has been implicated at the very onset of (weakly) turbulent flows, it is at present unclear how this chaotic attractor picture will fare for more complex fluid flows in which spatial decorrelation is observed [11]. Video feedback again provides an easily manipulated test-bed for studying two-dimensional "fluids" with complex local dynamics that are spatially incoherent. This section presents an example of the transition to fully developed video turbulence.

Photos 32, 33, 34, and 35 show this transition as a function of the strength of nonlinearity in the local dynamics. The latter maps the local intensity I through a cubic function $f(I) = h(I + bI^2 + cI^3)$ whose height h is the nonlinearity control parameter. The cubic function can be implemented with either an analog diode function generator or with a digital look up table. The first photo (32) shows the pattern at low nonlinearity: an inversion of the local intensity is seen; the pixel intensities visit a negative slope region of $f(x)$. This plus the 90 degree camera angle give rise to the alternating light-dark, four-fold symmetric pattern. At higher nonlinearity (photo 33) the smooth boundaries have broken down revealing smaller scale structure and limited local time-dependent behavior. The next photo (34) shows that large-scale structure has broken down entirely: spatial coherence is lost and the local dynamics is quite aperiodic. This is the analog of fully developed turbulence. The last photo (35), taken at yet higher nonlinearity, demonstrates homogeneous video turbulence in which the spatial scale of structure is smaller and the temporal frequencies are higher than the preceding photo.

A quantitative estimate of the complexity of such turbulence follows from a Kolmogorov eddy-scale argument. From this, the attractor dimension is approximately 2×10^3 and the information production rate, called the metric entropy, is approximately 6×10^4 bits per second.

X. Attractor-Basin Portraits for Two-Dimensional Maps

Somewhat amusingly, video feedback provides for the investigation of conventional nonlinear maps of the plane. A map $T: \mathbb{R}^2 \to \mathbb{R}^2$ of the plane $\mathbb{R}^2$ takes a point $\vec{x} = (x, y)$ into a new point $\vec{x}' = (x', y') = (f(x, y), g(x, y))$. The functions f and g implement a nonlinear distortion of the plane.

Since there are only two component variables rather than an entire screen full, these dynamical systems are much simpler than the spatially-extended systems to which video feedback is naturally adapted. If we identify the plane of a video image with the plane of states for a two-dimensional map, video feedback allows for the simultaneous simulation of (two-dimensional) *ensembles* of initial conditions. The basic image processing requirement is that the transformation effected by the feedback process warp the video raster in a nonlinear fashion prescribed by the two-dimensional mapping T. This is the essential function of the Rutt–Etra Video Synthesizer. This device is comprised of a set of video frequency locked oscillators that are used to drive the yoke of a modified monitor. The frequency, amplitude, and wave form of the oscillators determine the nonlinear raster transformation. The camera is simply directed at this monitor to close the feedback loop.

Photos 36 through 46 show some examples of the investigations that are readily performed with such a system. Here the only nonlinear processing of the video signal amplitude is clipping to black or white.

Photo 36 shows a chaotic attractor with characteristic folds and fractal structure. The latter appears as detailed filamentary structure. In video feedback, as in most experiments, the detail is truncated by finite resolution and noise. The mapping performed is a dissipative version of the area-preserving standard map [15].

Photos 37 and 38 show a piecewise-linear mapping due to Lozi [16]. At low nonlinearity there is a period 2 orbit. Photo 37 shows an ensemble's approach to this along a stable manifold with **homoclinic tangle** structure. A chaotic attractor at higher nonlinearity appears in Photo 38. Photos 39, 40, and 41 illustrate the approach of an ensemble of initial conditions to a period 4 attractor.

A period-doubling bifurcation sequence to chaos is shown in the next set of four photos (42, 43, 44, and 45) as a function of increasing nonlinearity. The sequence starts at a fixed point (42) which then becomes unstable (43) and

relaxes onto a period two limit cycle (44). Photo 45 shows a two "band" chaotic attractor later in the bifurcation sequence.

Finally, with constant illumination, rather than a brief initial burst of light, the basin of attraction can be investigated. Photo 46 demonstrates the basin for a simple period 2 limit cycle.

XI. Nonlinear Image Processing

This survey has given only a brief introduction to the contemporary study of spatially extended nonlinear dynamical systems. In this endeavor, video feedback is seen to be a flexible, high-speed simulator, on the one hand, and a source of diverse spatio-temporal experimental data, on the other. The survey has not described many other types of complex behavior, such as, how video feedback can be used to implement neural networks, spin glasses, and multiple-species chemical reactions. Space has also not allowed for a discussion of the theoretical relationship between information and dynamical systems theories that are so important in the analysis of this complexity [17]. We will close with a discussion of the relationship of this work to future directions in nonlinear image processing.

Some similarities with image processing systems are clear from the mathematical formulation of the models and from the video apparatus. The systems we have studied here are *nonlinear iterative* image processing systems. The diversity of behavior seen in video feedback indicates that incorporating both nonlinearity and iteration will lead to many new image processing techniques and to a broader theoretical framework for image processing based on dynamical systems theory. From the point of view of dynamical systems, image processing tasks suggest questions of how to design the attractors and basin structures of spatially extended dynamical systems to perform specific computation and image processing tasks and how to do these efficiently.

From a slightly different perspective, video feedback as presented here is an experimental exploration of the potentials of optical computing. The camera–monitor system is employed essentially as an image operational amplifier. As far as the methodology and the phenomena are concerned any technology could be used for this function. To date there appear to be no reasonable alternative optical op amps. If such an instrumentation-quality device were to become available, especially one that was truly parallel in operation then, for the investigation of two- and higher dimensional spatial dynamics, feedback optical computing would vastly outstrip digital computers of any architecture in speed and ease-of-use. The potential impact on the simulation of very complex scientific problems is hard to overestimate. Even with current video technology substantial progress along these lines could be made. The manufacturers of broadcast quality and high definition television (HDTV) video equipment are in unique positions to establish laboratories for video feedback investigations of nonlinear spatially extended dynamics.

It is somewhat sobering to realize that the diversity of phenomena presented here could have been as easily investigated thirty years ago as now. The basic technology for video feedback has been available since the 1950's. If history is any indication, then, the alternative approach advocated here may be a route not taken. Despite their potential for scientific simulation, video feedback and related image processing techniques could very well continue to be eclipsed by expensive multiple-processor supercomputers. The resurgence in interest in optical computing, in distributed processing, and in parallel computational architectures, however, are hopeful signs that interactive, high-speed machines for the experimental mathematical investigation of complexity may be widely available in the next decade. The next few years will tell if image processing and video feedback contribute directly to this line of technological development.

Acknowledgment

This work has benefited greatly from the expertise of Donald Day of the California College of Arts and Crafts. The two-dimensional mapping work was done in CCAC's Video Department.

References

[1] J. Gleick, *Chaos, Making a New Science*. New York: Viking, 1987.
[2] P. Berge, Y. Pomeau, and C. Vidal, *Order within Chaos: Towards a Deterministic Approach to Turbulence*. New York: Wiley, 1984.
[3] J. P. Crutchfield, N. H. Packard, J. D. Farmer, and R. S. Shaw, "Chaos," *Sci. Am.* 255, vol. 46, Dec. 1986.
[4] D. Campbell, J. P. Crutchfield, J. D. Farmer, and E. Jen, "Experimental mathematics: The role of computation in nonlinear studies," *Comm. ACM*, vol. 28, p. 374, 1985.
[5] J. P. Crutchfield, "Space-time dynamics in video feedback," *Physica* vol. 10D, p. 229, 1984.
[6] J. P. Crutchfield and K. Kaneko, "Phenomenology of spatio-temporal chaos" in *Directions in Chaos*, (Hao Bai-Lin, Ed.) Singapore: World Scientific Publishers, 1987.
[7] J. P. Crutchfield, *Space-Time Dynamics in Video Feedback and Chaotic Attractors of Driven Oscillators*, video tape, Aerial Press, P.O. Box 1360, Santa Cruz, CA 95064, 1984.
[8] Pixel processing was performed by an analog image processor designed by Dan Sandin of the University of Illinois, Chicago Circle, and by a max video digital image processor manufactured by Datacube, Inc. (Peabody, MA).
[9] For this we have used a Ruti–Etra Video Synthesizer. While these are no longer manufactured, modern digital video effects machines do incorporate similar raster manipulation functions. Quantel's *Mirage*, Ampex's *ADO*, and the more recent Sony *Real-Time Texture-Mapping System* are examples. For the latter see M. Oka, K. Tsutsui, A. Ohba, Y. Kurauchi, and T. Tago, "Real-time manipulation of texture-mapped surfaces," *Comp. Graphics*, vol. 21, 181, 1987.
[10] A. M. Turing, "The chemical basis of morphogenesis," *Trans. Roy. Soc., Series B*, vol. 237, p. 5, 1952.
[11] J. Crutchfield and K. Kaneko, "Are attractors relevant to turbulence?," submitted to *Phys. Rev. Lett.*, 1988.
[12] For this and other examples, see A. T. Winfree, *The Geometry of Biological Time*, Berlin: Springer-Verlag, 1980.
[13] cf. K. I. Agladze and V. I. Krinsky, "Multi-armed vortices in an active chemical medium," *Nature*, vol. 296, p. 242, 1982.
[14] D. J. Tritton, *Physical Fluid Dynamics*, New York: Van Nostrand Reinhold, 1977.
[15] A. J. Lieberman and M. A. Lichtenberg, *Regular and Stochastic Motion*. New York: Springer-Verlag, 1983.
[16] R. Lozi, *J. Phys.*, vol. 39, C5-9, 1978.
[17] J. P. Crutchfield and B. S. McNamara, "Equations of motion from a data series," *Complex Systems*, vol. 1, p. 417, 1987.

Photo 1. A fixed point attractor.

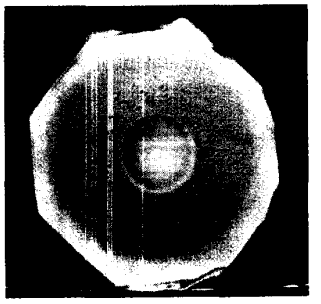

Photo 2. Snapshot of a limit cycle attractor.

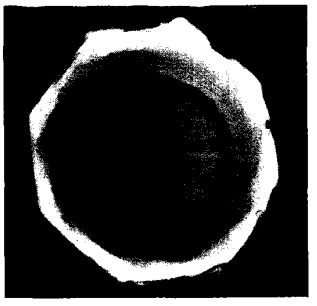

Photo 3. A snapshot at a later time; the central region has grown.

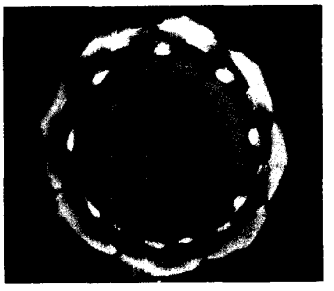

Photo 4. A snapshot of the limit cycle attractor as the state collapses back to a uniform pattern.

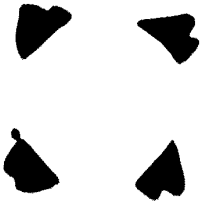

Photo 5. Chaotic attractor in a symmetry-locking regime: a snapshot when the state is near a fourfold symmetric pattern.

Photo 6. Transit from a four- to twenty-one-fold symmetric pattern.

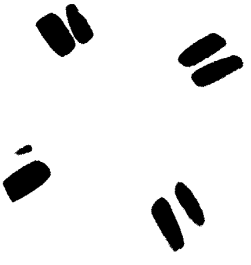

Photo 7. Another intermediate state in the transition.

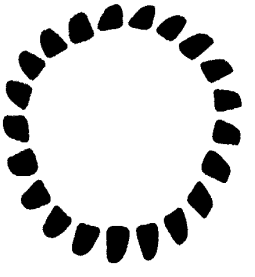

Photo 8. Near the twenty-one-fold symmetric, unstable fixed point pattern.

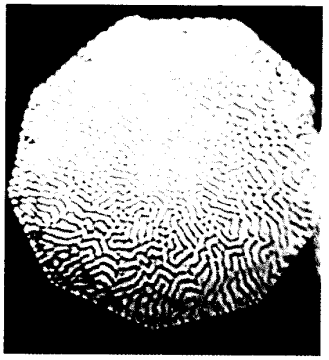

Photo 9. Snapshot of a *gas* of video dislocations.

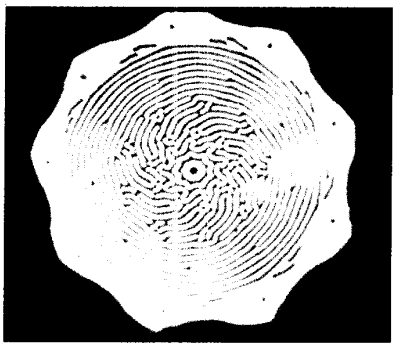

Photo 10. Dislocations are created at the center and move out into the laminar region where they are annihilated.

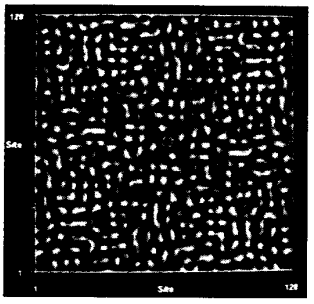

Photo 11. Numerical model of dislocations: 20 steps after starting from a random initial pattern.

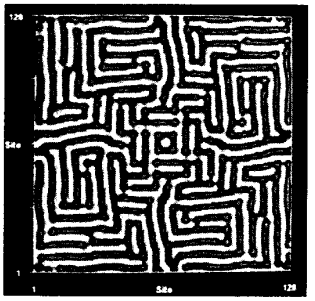

Photo 12. At 200 time steps domains of parallel fingers appear.

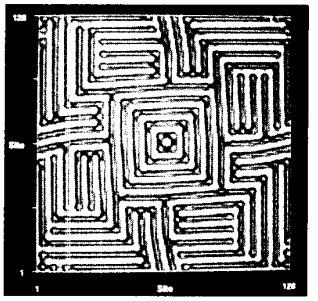

Photo 13. At 1100 steps the domains have increased in size and begin to organize into concentric rings.

Photo 14. One-armed spiral wave.

Photo 15. Two-armed spiral wave.

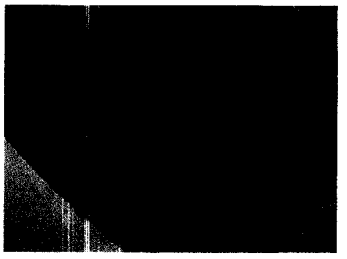

Photo 16. Three-armed spiral wave.

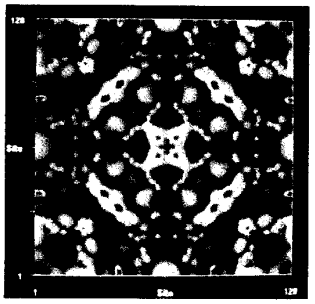

Photo 17. Transient spatial chaos 310 steps after a single-site perturbed initial pattern.

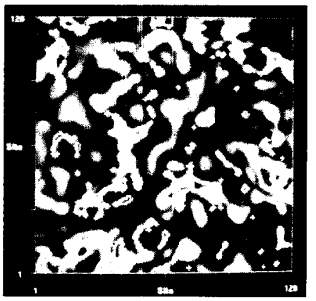

Photo 18. Transient spatial chaos 492 steps after a random initial pattern.

Photo 19. Logarithmic spiral.

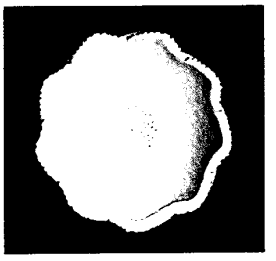

Photo 20. Phyllotaxic symmetry in a crystalline dot-lattice.

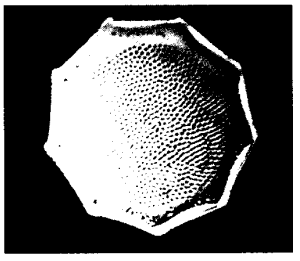

Photo 21. Crystalline dot-lattice with locally symmetric domains separated by walls.

Photo 22. Spatial amplification of fluctuations in a video waterfall.

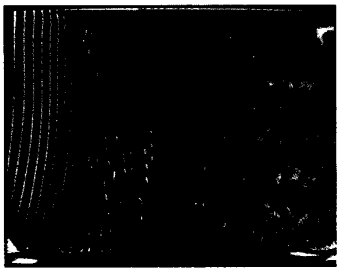

Photo 23. Growth of a small perturbation at the photo's right side.

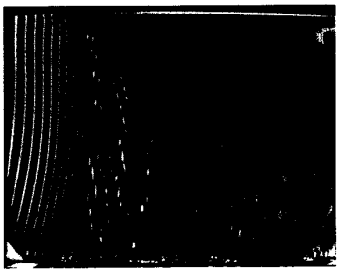

Photo 24. Downscreen propagation of the now macroscopic structure.

Photo 25. One amplification pathway for a noise-driven relaxation oscillator.

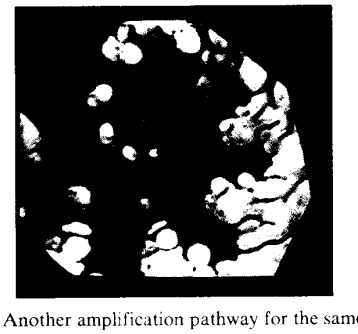

Photo 26. Another amplification pathway for the same oscillator.

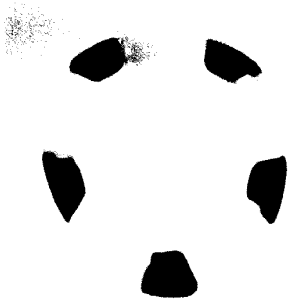

Photo 27. Symmetry-locking bifurcation: counterclockwise rotating, fivefold symmtric pattern.

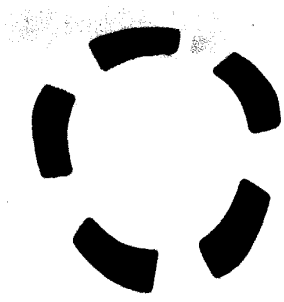

Photo 28. At slightly increased camera angle: a stationary fivefold pattern.

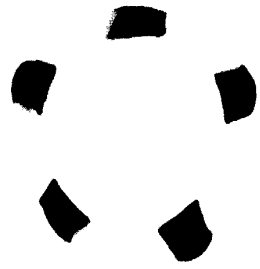

Photo 29. The fivefold pattern begins to move clockwise at increased angle.

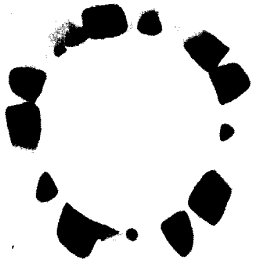

Photo 30. Instability at the bifurcation to thirteenfold symmetry.

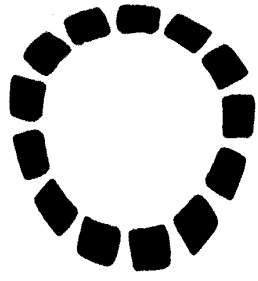

Photo 31. The thirteenfold, stable fixed point pattern.

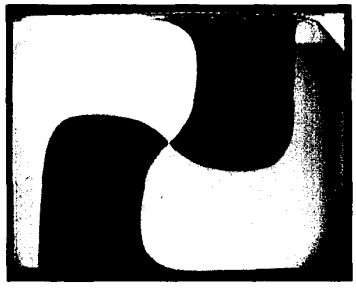

Photo 32. Below the transition to video turbulence: a stable fixed point pattern.

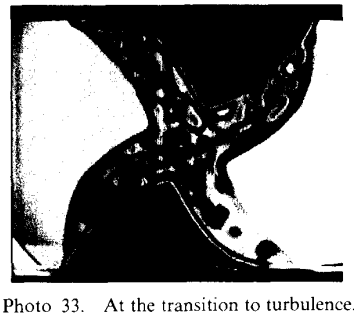

Photo 33. At the transition to turbulence.

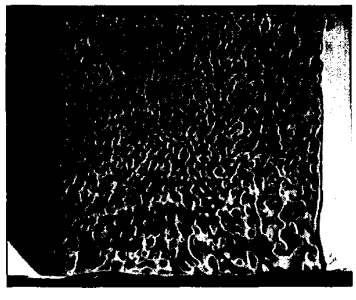

Photo 34. Spatial coherence is lost at higher nonlinearity: fully developed video turbulence sets in.

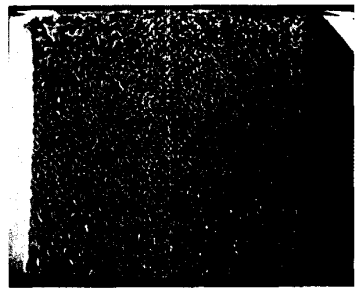

Photo 35. Homogeneous video turbulence with very small eddy size.

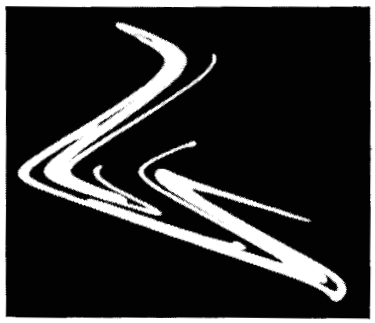

Photo 36. Chaotic attractor in two dimensions.

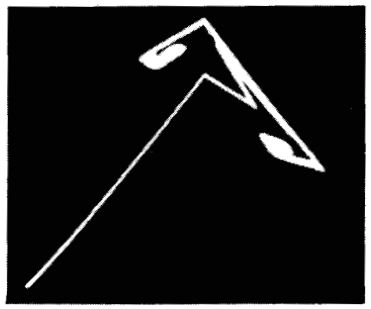

Photo 37. Transients flow along a stable manifold exhibiting "homoclinic tangle" structure.

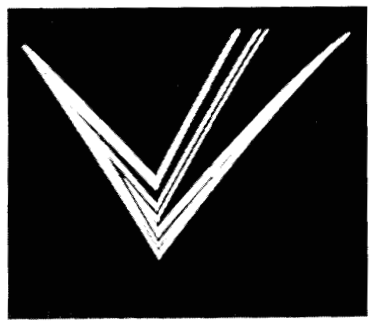

Photo 38. Piecewise-linear chaotic attractor.

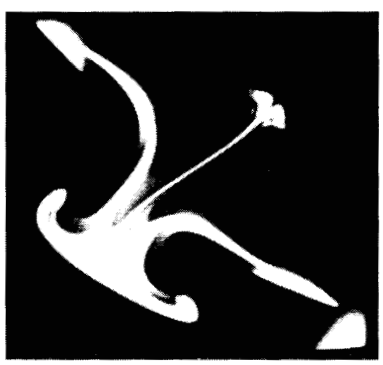

Photo 39. Initial stage of a relaxation to a period-four limit cycle.

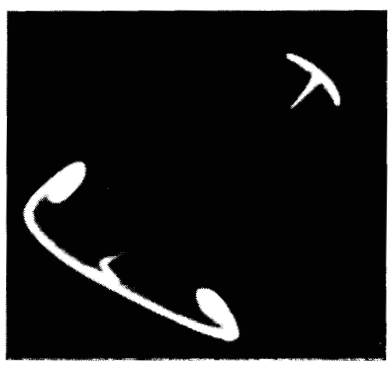

Photo 40. Later in the relaxation process.

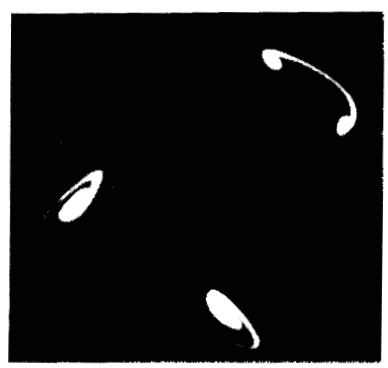

Photo 41. Relaxation almost complete: the points on the period-four limit cycle are discernible.

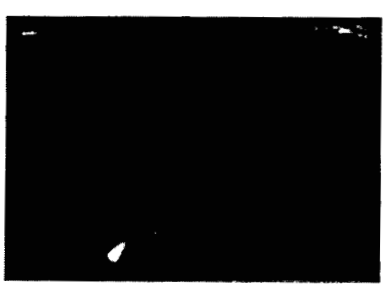

Photo 42. The period-doubling bifurcation to chaos starts at a fixed point.

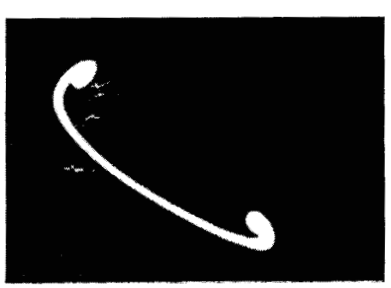

Photo 43. The fixed-point looses stability and the system relaxes onto a stable period two limit cycle.

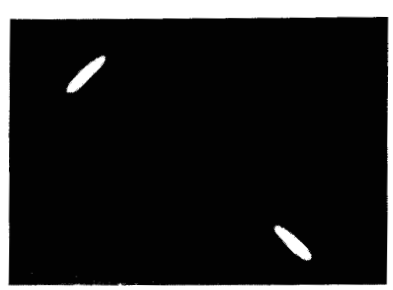

Photo 44. The period two limit cycle.

Photo 45. A two-band chaotic attractor later in the bifurcation sequence.

Photo 46. Basin of attraction for period-two limit cycle.